

# Modelling of the Hungarian spread of COVID-19 and control strategies with risk-based approach

3 **Zsuzsa Farkas<sup>1\*</sup>, Tekla Engelhardt<sup>1</sup>, Erika Ország<sup>1</sup>, Miklós Süth<sup>1</sup>, Szilveszter Csorba<sup>1</sup>, Ákos**  
4 **Bernard Jóźwiak<sup>1</sup>**

<sup>1</sup>University of Veterinary Medicine Budapest, Digital Food Chain Education, Research, Development and Innovation Institute, H-1078 Budapest, István utca 2., Hungary

7    **\* Correspondence:**

8 Corresponding Author

9 [farkas.zsuzsa@univet.hu](mailto:farkas.zsuzsa@univet.hu)

## **Abstract**

## **Background**

Novel Coronavirus Disease (COVID-19), caused by Severe Acute Respiratory Syndrome Coronavirus 2 (SARS-CoV-2), threatens humanity in terms of health and economy as it spreads extremely fast and causes massive epidemics all over the world. In the absence of a vaccine, social isolation and hygienic measures are the only way to curb the virus.

## **Methods**

In our study, the Hungarian spread of COVID-19 is modelled by applying a modified SEIR (Susceptible, Exposed, Infected, Recovered) compartment model, which takes into account the route of disease transmission not only from infected, but from latent individuals (exposed compartment) as well. The differences between the modified model and the traditional SEIR model has been evaluated. The different scenarios of disease spreading simulate the effect of the different level of interventions (social distancing and hygienic measures) taken place in Hungary. The modelling also considers the population and mobility data which are also essential in case of infectious disease spreading. For controlling the disease in the long-term a network-based analysis is provided based on the concept of the epidemic threshold and the identification of super-spreader population groups.

## **Results**

According to sensitivity analysis of the modified SEIR model, disease transmission of latent individuals has the greatest effect on the number of infections. Based on the results, the applied interventions have a great impact on the disease spreading and are effective in controlling the COVID-19 epidemic., a network-based analysis is provided based on the concept of the epidemic threshold and the identification of super-spreader population groups. According to the results of the network-based study, the proportion of people to be sampled for an effective disease control is the function of the identified people with high number of contacts in social networks who act as super-spreaders.

## **Conclusion**

Applying network-based random, selective and targeted sampling, testing and isolation of affected individuals would yield significantly different sample sizes, highlighting the importance of super-spreaders. Network analysis (but also all computational science methods) need large amount of good quality data and the spread of these methods could be supported by easy-to-use tools. We wanted to raise awareness also on this issue.

**Keywords:** COVID-19, epidemiological modelling, control strategies, risk-based testing, super-spreader identification, network analysis.

## 47 Background

48 Genetic mutations of microorganisms are inevitable, however, due to climate crisis and other crucial  
49 drivers of change, emerging infectious diseases are more and more likely to threaten humanity in the  
50 near future. Nowadays, mankind is in a great crisis in terms of health and economy because of an  
51 epidemic caused by the mutation of an originally animal-related coronavirus (1)(2). By adapting to  
52 humans, the virus named Severe Acute Respiratory Syndrome Coronavirus 2 (SARS-CoV-2) (3)  
53 caused pandemic infectious disease COVID-19 (4) that affects millions of lives. As of today, it has  
54 appeared almost all over the world, it spreads extremely fast and causes massive epidemics.

55 COVID-19 is transmitted by inhalation or contact with infected droplets (5,6). It must be noted that  
56 the aerosol and surface stability of SARS-CoV-2 is higher than SARS-CoV-1, therefore indirect  
57 transmission routes are more significant than previously thought (7,8).

58 In the absence of a vaccine, social isolation and hygienic measures are the only way to curb the virus.  
59 However, these interventions are proved to be effective only when applied very strictly because of  
60 the very high virulence of SARS-CoV-2 (9,10). The level of isolation needed (e.g. school closures,  
61 banned events and gatherings) is such high that it is unsustainable in the long run.

62 Modelling is a key option in epidemiology in cases when limited data are available regarding an  
63 infectious disease like emerging diseases such as COVID-19. Scenario analysis is a tool by which  
64 information can be gained that can support decision making regarding mitigation strategies and risk  
65 management, nevertheless, it has its limitations which must be taken into account. As of today,  
66 several publications have already appeared which have attempted to simulate the spread of COVID-  
67 19 from different aspects. Most of the earliest publications study the epidemic in China by applying  
68 the SEIR (Susceptible, Exposed, Infected, Recovered) compartment model with different  
69 modifications depending on the purpose of the modelling. Some publications try to estimate the  
70 extent of the epidemic regarding time period and number of total infections (11,12), while most of  
71 the studies model the effect of interventions such as isolation and quarantine (13–18).

72 As time goes by, more and more information is available regarding the disease dynamics and disease  
73 characteristics of COVID-19, thereby epidemiological models and parameters of the models can  
74 more precisely be determined. One of the most important finding is that there are many latent people  
75 who develop no symptoms or only mild symptoms, and the disease is infectious in the latent phase as  
76 well. Therefore, many people carry and transmit the virus, thereby contribute to the spread of the  
77 disease in an unnoticeable way (19–23). Most of the earlier research did not account for this type of  
78 transmission because of the lack of knowledge, though it would be essential in understanding the  
79 disease dynamics (24).

80 Conventional compartment models try to capture state transitions and simulate the course of disease  
81 in a uniform and homogenous population. However, the basic assumption that any person can contact  
82 anyone, and everyone has the same number of contacts, is not true in the real social networks.

83 Many real networks share same characteristics and are surprisingly similar to each other. These  
84 networks are sparse, where many nodes with small number of contacts are connected with each other  
85 through few large hubs with many contacts. The number of contacts a node has is denoted by  $k$ , and  
86 is called the degree of the node. If the degree distribution of a network follows a power law, it is  
87 called a *scale-free network* (25). In scale-free networks, compared to random networks, nodes can  
88 have very different degrees, ranging from very small, to huge (which are called hubs). Thus, the  
89 average degree is not enough in itself to describe the network topology. Diseases can spread much

faster in such networks due to the presence of super-spreader hubs. These networks are also known for their specific robustness: they withstand untargeted attacks without falling apart, but they are vulnerable to attacks targeting the large hubs of the network. This phenomenon could also be used for planning targeted interventions.

The aim of this study is to present an epidemiological modelling based on the SEIR compartment model that is generally accepted for modelling the spread of COVID-19, but with a modification in order to take the transmission route of the latent, yet infectious people into account. Network analysis-based intervention strategies are also discussed in the paper, since the profound implications of network theory are not widely known in the public health community.

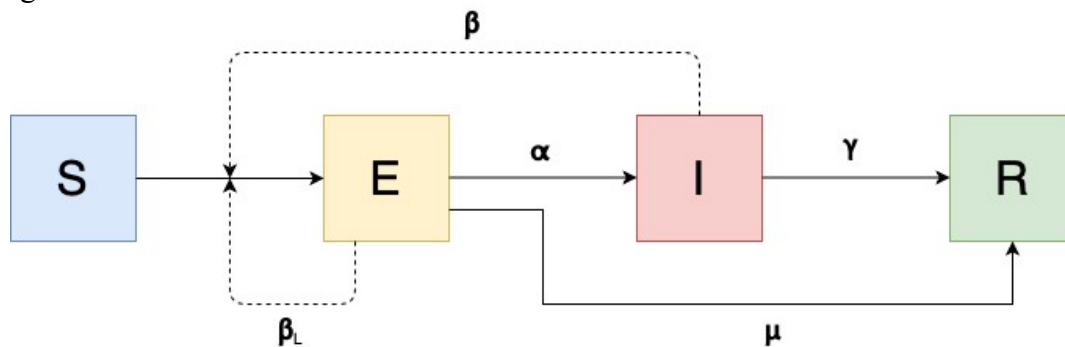
## Materials and Methods

### Structure of the epidemiological model

#### Modified SEIR model for COVID-19

For COVID-19, we have built a SEIR (Susceptible, Exposed, Infected, Recovered) compartment model for a basis of the modelling but we have applied some modifications. In the original SEIR model, the Exposed compartment is not infectious. Our modified SEIR model accounts for the infectiousness of this compartment ‘E’, as it has been shown by previous studies (19–23), and also account for a route of transition of being recovered without symptoms or with mild symptoms from the Exposed compartment to the Recovered compartment. For better differentiation from the original, SEIR model with the applied modifications will be referred as ‘modified SEIR model’ (Figure 1.), and individuals in Exposed compartment are called ‘latent’.

Figure 1



Structure of the modified SEIR model with compartment initials (Susceptible, Exposed (Latent), Infected, Recovered), transitions from one compartment to another (full line), parameters and routes of infection (dashed line). Susceptible individuals can get the infection either from individuals being in the Infected compartment with the rate of  $\beta$ , or from Exposed compartment (latent individuals) with the rate of  $\beta_L$ .

The following differential equations describe the dynamics of the modified SEIR model (1):

$$\begin{aligned}
120 \quad & \frac{dS}{dt} = -\beta_L SE - \beta SI, \\
121 \quad & \frac{dE}{dt} = \beta_L SE + \beta SI - \alpha E - \mu E, \\
122 \quad & \frac{dI}{dt} = \alpha E - \gamma I \\
123 \quad & \frac{dR}{dt} = \gamma I + \mu E \quad (1)
\end{aligned}$$

124 where S, E, I and R are the fractions of Susceptible, Exposed, Infected and Recovered individuals,  
125 and  $S+E+I+R=1$  at all times.

## 126 Parameters of the model

127 Selection of values for different model parameters has been done by literature research. There were  
128 many estimations in previous publications for the value of basic reproduction number,  $R_0$ , ranging  
129 from 1.95 (1.4-2.5) (26) to 6.47 (95% CI 5.71–7.23) (27). Our model has been built to be consistent  
130 with the average range of reported  $R_0$  values. The mean value of the incubation period was  
131 consistently around 4 to 6 days in numerous publications (12,28–31), therefore we selected the  
132 number of latent days to be 5 (transition rate from Exposed compartment to Infected compartment).  
133 3.5 days of infectious period was chosen for the calculation of recovery rate, following the studies of  
134 Li et al. (19) and Tang et al. (27). The transition rate from Exposed compartment to Recovered  
135 compartment arises from the number of days latent individuals spend while carrying and transmitting  
136 the virus, which in our model is the sum of incubation period and infectious period, therefor 8.5 days.

137 The parameter values in the baseline scenario (*Scenario 1*) with no interventions are shown in Table  
138 1.

139 Table 1. Definitions and values of the modified SEIR model parameters

	Definition	Number of days	Value (day <sup>-1</sup> )
$\alpha$	Transition rate from Exposed compartment to Infected compartment	5	0.2
$\gamma$	Recovery rate	3.5	0.29
$\mu$	Transition rate from Exposed compartment to Recovered compartment	8.5	0.12
$\beta$	Transmission rate		0.8*
$\beta_L$	Latent transmission rate		0.4*

140 \*Approximate values considered to be in line with the average reported  $R_0$  values (32,33). These parameters will change  
141 in Scenarios 2 and 3.

142  
143 According to Wu et al. (18) and Nishiura et al. (21), latent individuals are able to transmit the  
144 infection 50% less than infected individuals. This is in line with other studies regarding

145 asymptomatic transmission rate of 50% in case of influenza (34,35). Therefore, the rate  $\beta_L$  (beta  
146 latent) will be half of the  $\beta$  value.

147

## 148 **Limitations of the compartment model**

149 The formulation was made assuming that natural birth rate is equal to natural mortality rate, therefore  
150 the observed dynamics are considered to be caused by the disease. Individual differences, that could  
151 influence the susceptibility of people such as age, gender, general health condition cannot be taken  
152 into account, all individuals are considered equally susceptible for the disease.

## 153 **GLEAMviz software**

154 Simulations were performed with the publicly available GLEAMviz Simulation System (36), that is a  
155 scientific application designed for performing simulations of the spread of infectious diseases. With  
156 the real-world demographic and mobility data, location and time of potential virus transmission by  
157 human interactions can be simulated. Compartment model in the Simulation System is customizable,  
158 thereby can be adapted for various infectious diseases. The spread of the infection among individuals  
159 is driven by the characteristics of the disease specified in the compartment model (37–39).

## 160 **Setting options regarding compartment models in GLEAMviz**

161 Number of compartments and transitions from one compartment to another (infectious or  
162 spontaneous) can arbitrarily be defined. In case of each compartment, air travel and commuting can  
163 be allowed or disallowed and there are 3 ways for the settings of infectiousness for each  
164 compartment: 1. Carrier 2. Clinical 3. None.

## 165 **Other setting options in GLEAMviz**

166 Simulations can be done with single run or multiple runs, in latter case, the number of runs can be  
167 defined, and the results can be retrieved with median and confidence interval values calculated over  
168 the set of runs. Start date and duration of the simulation can be set. GLEAM uses robust statistical  
169 methods and executes the simulation in a sequence of time steps that represents full days. Average  
170 percentage of airline traffic can be set. For each simulated flight, the number of passengers is a  
171 stochastic variable sampled from a binomial distribution whose mean is given by the airline traffic  
172 value times the number of bookings. There is an option for enabling seasonality with a built-in  
173 algorithm that rescales the basic reproduction ratio  $R_0$  by a sinusoidal function. For commuting  
174 model, one can choose from gravity (40) or radiation (41) models. Users can set the average number  
175 of hours spent by the commuters at the commuting destination. The default value is 8 hours (the  
176 average amount of working time in a day). Minimum number of clinical cases that need to occur in a  
177 country for it to be considered infected and minimum number of infected countries for a global  
178 epidemic to be considered to occur can be set. Initial population composition for each compartment  
179 can be specified in percentages of the total global population. Initial epidemic locations (cities) and  
180 number of individuals in the given compartment can be defined for arbitrary number of initial  
181 epidemic seeds.

182 The so-called ‘exceptions’ panel in GLEAMviz provides a way to specify time and space dependent  
183 changes of the variable values defined in the compartment model. Each exception lets the user define  
184 alternative values for one or more variables for a specified period and specified areas (e.g. cities,  
185 countries).

186

## 187 **Basic scenarios for modelling disease spread in Hungary with interventions**

### 188 **Scenario 1 – ‘worst case’**

189 Worst case scenario with no specific interventions, model parameters determined in the above section  
190 ‘Parameters of the model’. It represents the conditions of the beginning of the epidemic in Hungary  
191 (04 March 2020) (COVID-19 pandemic in Hungary, 2020). It is assumed that only infected  
192 individuals with serious and founded COVID-19 symptoms are quarantined in Hungary.

193 Regarding interventions, our assumption is that all interventions applied (social isolation and  
194 hygienic measures) overall decrease the rate of virus transmission, in our case  $\beta$  and  $\beta_L$  values which  
195 is in line with the theory of Li et al. (19) and Ferguson et al. (15). Therefore, in case of scenarios with  
196 interventions (Scenarios 2, 3), only these parameter values are decreased proportionally depending on  
197 the extent of the effect of interventions.

### 198 **Scenario 2 – First round of interventions**

199 In Hungary, from 16 March 2020, schools and universities operate by distance-learning, nursery  
200 schools and other pre-school establishments only provide duty service, more and more employers  
201 provide the opportunity of home office for the workers and people are getting conscious about  
202 staying at home and reducing the physical contacts as much as possible. Events with large number of  
203 people were banned (the limit was 100 people for indoor and 500 for outdoor events, respectively).  
204 According to our assumption that is supported by the data of Google Analytics (42) and Hungarian  
205 traffic statistics (43), that means a 50% decrease in the level of social interactions compared to the  
206 normal lifestyle. This, together with the raised awareness of the disease and the importance of  
207 detection and quarantine of infected people, based on the approach of Ferguson et al. (15) results in  
208 the decrease of  $\beta$  and  $\beta_L$  values to 0.4 and 0.2 (from 0.8 and 0.4), respectively.

### 209 **Scenario 3 – Second round of interventions**

210 From 28 March, the Hungarian government have ordered curfew restrictions across the country, in  
211 the first round until the 11<sup>th</sup> of April, and in the second round it was extended for an indefinite period.  
212 The goal of the restrictions was generally to limit the contact of people who do not live in the same  
213 household, therefore residences should only be left for the satisfaction of basic needs (e.g. work,  
214 grocery, pharmacy, health services) the previously specified restrictions regarding the institutions  
215 have remained unchanged. According to our assumption and the further mentioned references (42,43)  
216 that resulted in a further 25%, altogether 75% reduction in the level of social interactions compared  
217 to the normal lifestyle, which means a reduction in  $\beta$  and  $\beta_L$  values to 0.3 and 0.1, respectively.

218 Scenarios 1 to 3 attempt to model the real-life situation regarding disease spreading with the  
219 temporally applied intervention measures in Hungary. It is noted, however, that the list of  
220 interventions is not fully complete, only those are mentioned which are crucial regarding scenario  
221 building.

### 222 **Practical implementation in GLEAMviz (Settings)**

223 Unless not specifically indicated, settings are applied for each four Scenarios.

‘MODEL’ panel: Modified SEIR model (Figure 1.) with parameters defined in section ‘Parameters of the model’. Special GLEAMviz setting options for different compartments are shown in Table 2.

Table 2. Special GLEAMviz setting options in different compartments

	Susceptible	Exposed (Latent)	Infected	Recovered
Infectiousness	none	carrier*	clinical**	none
Commuting	allowed	allowed	disallowed	allowed
Air travel	allowed	allowed	disallowed	allowed

\*: *but transmitting the virus with the rate of  $\beta_L$*

\*\*.: *transmitting the virus with the rate of  $\beta$*

‘SETTINGS’ panel:

- Multi-run simulation (20 runs, the maximum possible number of runs)
  - Start date: 4 March 2020 - the date of the first reported cases of SARS-CoV-2 infection (44)
  - Airline traffic:
    - *Scenario 1*: 88% (12% decrease globally in the first half of March according to OAG statistics) (45)
    - *Scenario 2*: 52% (48% decrease globally in the second half of March) (45)
    - *Scenario 3*: 30% (66% decrease rounded up to 70% as data were available only until 20 April 2020)(45)
  - Commuting model: radiation model was chosen as it is proved to describe the commuting patterns better when parameter-free algorithms must be used (41,46).
  - Time spent at commuting destination:
    - *Scenario 1*: 8 hours (default, assuming no change at commuting in Hungarian region)
    - *Scenario 2*: 4 hours (50% reduction in commuting according to Hungarian traffic statistic)(42,43)
    - *Scenario 3*: time spent at commuting destination: 2 hours (75% reduction in commuting according to Hungarian traffic statistic) (42,43)
  - Seasonality: disabled – as it is believed that SARS-CoV-2 is not affected by weather parameters and there is no evidence to the contrary at the moment (47).
  - Minimum number of clinical cases that need to occur in a country for it to be considered infected: 1 (default)
  - Minimum number of infected countries for an occurrence to be an epidemic: 2 (default)
  - Initial global distribution of a population in compartments: 100% susceptible
  - Initial geographic location of the epidemic: Officially 2 infected people were registered on the 4<sup>th</sup> of March 2020 in Hungary (48), Budapest, but in order to get more realistic simulations regarding the coverage of the region, initially 5 infected individuals were set for Budapest and 3, 3 latent individuals for Debrecen and lake Balaton, based on population data, respectively. These were the only available locations in GLEAMviz software for Hungary.
- As there is a possibility for setting numerous initial locations of the epidemic, number of individuals with registered COVID-19 infections (number of active patients) were collected for the 4<sup>th</sup> of March, 2020. Only cities can be set in the software, and data about registered



infections were available in different levels of aggregation. Table 3. shows the initial locations with number of infected people used in the simulation (only >20) apart from Hungary.

Table 3. Initial locations and number of infected individuals (apart from Hungary) set in GLEAMviz.

Initial location		No. of infected individuals	Level of aggregation of the data	Reference
Country	City			
Austria	Innsbruck	22	national (halved)	(49)
	Vienna	21	national (halved)	
France	Lille	65	regional	(50)
	Lyon	49	regional	
	Strasbourg	38	regional	
	Paris	55	regional	
Germany	Düsseldorf	115	federal state	(51)
	Munich	48	federal state	
	Stuttgart	50	federal state	
Italy	Ancona	80	regional	(52)
	Bologna	516	regional	
	Florence	37	regional	
	Milan	1497	regional	
	Naples	31	regional	
	Rome	27	regional	
	Turin	82	regional	
	Venice	345	regional	
Spain	Barcelona	24	autonomous community	(53)
	Madrid	90	autonomous community	
China	Beijing	1267	national except Hubei	(54)
	Wuhan	24085	Hubei province	
Iran	Tehran	2259	national	(54)
Japan	Tokyo	278	national	(55)
Singapore	Singapore	33	national	(56)
South Korea	Seoul	5547	national	(57)

266 Settings of ‘EXCEPTIONS’ panel are shown in Table 4.

267 Table 4. ‘EXCEPTIONS’ panel settings in GLEAMviz.

No. of Scenario	Exception(s) applied	
<i>Scenario 1</i>	No exceptions applied	
<i>Scenario 2</i>	$\beta = 0.4$ ; $\beta_L = 0.2$ ; from 16 March 2020 till the end of the simulation; in the Hungarian region	
<i>Scenario 3</i>	$\beta = 0.4$ ; $\beta_L = 0.2$ ; from 16 March 2020 to 27 March 2020; in the Hungarian region	$\beta = 0.3$ ; $\beta_L = 0.1$ ; from 28 March 2020 till the end of the simulation; in the Hungarian region

268

## 269 Comparison of modified SEIR model with traditional SEIR model

270 In order to evaluate the differences between modified SEIR model and the traditional (‘basic’) SEIR  
 271 model, a simulation has been made in which parameters  $\beta_L$  and  $\mu$  were disregarded (transition rates  
 272 that contribute to the infectiousness of exposed individuals). Other parameters and settings were the  
 273 same as in Scenario 1 in the simulation.

## 274 Sensitivity analysis of modified SEIR model

275 The sensitivity analysis has been done to reveal the parameter(s) to which the model is the most  
 276 sensitive. There were five parameters in our modified SEIR model to be investigated:  $\beta$ ,  $\beta_L$ ,  $\gamma$ ,  $\alpha$ ,  $\mu$ .  
 277 The parameters and settings of *Scenario 1* was used for the evaluation. The maximum value of the  
 278 daily number of individuals in the infected compartment and the number of days related to this value  
 279 were selected as the endpoint. Only one parameter per scenario was changed at a time. Changes in  
 280 both directions were evaluated with lower ( $\times \frac{1}{2}$ ) and higher ( $\times 2$ ) values compared to the baseline  
 281 value (Table 1.) of the examined parameter.

## 282 Network analysis-based intervention strategies

283 The basic assumption of the conventional compartment models is that any person can contact  
 284 anyone, and everyone has the same number of contacts, is not true in the real contact networks. Real  
 285 networks are sparse, where many nodes with small number of contacts are connected with each other  
 286 through few large hubs with many contacts, which could also be identified as super-spreaders.

287 The first applications of network science to disease modelling set a new scientific field called  
 288 network epidemics (58). When modelling disease spreading, the network characteristics will yield  
 289 many important differences compared to the conventional compartment models.

290 First of all, the diseases spread much faster in scale free networks due to the presence of hubs. In  
 291 network epidemics the concept of *epidemic threshold* ( $\lambda_c$ ) is used: pathogens can only spread if the  
 292 spreading rate  $\lambda$  exceeds  $\lambda_c$ . The spreading rate can be defined as:

$$293 \quad \lambda = \frac{\beta^*}{\mu} \quad (2)$$

where  $\beta^*$  is the likelihood that the disease will be transmitted from one infected person to a susceptible one in a unit of time, and  $\mu$  is the recovery rate. The conventional  $R_0$  can be defined as:

$$R_0 = \langle k \rangle \lambda \quad (3)$$

where  $\langle k \rangle$  is the average degree. In case of scale free networks, the epidemic threshold is:

$$\lambda_c = \frac{1}{\frac{\langle k^2 \rangle}{\langle k \rangle} - 1} \quad (4)$$

where  $\langle k^2 \rangle$  is the second moment of the degree distribution, and it is used in the calculation of the variance (25). In scale free networks,  $\langle k^2 \rangle$  is significantly larger than  $\langle k \rangle$ , due to the huge variance in degrees of the nodes. This means, that in large scale-free networks  $\lambda_c$  is very small, meaning that most of the diseases can spread very rapidly because of the presence of large hubs. This holds for every network (not only scale-free ones), where there is a large difference between the degrees of the nodes. This phenomenon was also captured by Meyers et al. (59), who applied the methods of contact network epidemiology for SARS, to illustrate that for a single value of  $R_0$ , any two outbreaks, even in the same setting, may have very different epidemiological outcomes.

Many social contact networks are also scale-free networks. We don't have a map of the Hungarian contact network of people, but we can estimate  $\lambda_c$  with the use of other data. The Copenhagen Networks Study resulted in a multi-layer temporal network which connects a population of more than 700 university students over a period of four weeks (60). We have used a 2-week (common agreed suggested quarantine period)(61) subset of the network of physical proximity among the participants (estimated via Bluetooth signal strength) to simulate direct personal contacts. We have used the settings defined by Stopczynski et al. (62): only contacts where the signal strength was  $\geq -75$  dBm were used, corresponding to distances of approximately 1 meter or less. Based on these data, a network had been constructed and analysed with the use of KNIME free and open-source data analytics (63), reporting and integration platform and igraph R-package (64).

Other important consequence of network topology is the difference in planning intervention strategies. If we try to remove nodes from the network either with immunization (which we can't perform yet in case of COVID-19) or with identifying latent and infected people with sampling and testing, and then removing them with quarantine measures, we may have use other than conventional options as well. For assessing the effect of identifying and removing latent and infected people with sampling, testing and consequent quarantine measures, we use the concept of critical immunization well established in network epidemiology. Critical immunization  $g_c$  is the proportion of nodes needed to be removed from the network to stop the spreading of the disease.

### 325 *Random sampling*

In case of random sampling, testing (and consequent removing of SARS-CoV-2 positive people from the contact network), the critical immunization  $g_c$  can be defined as:

$$g_c = 1 - \frac{\lambda_c}{\lambda} \quad (5)$$

Besides random sampling, there are other options as well, stemming from the characteristic of the scale free networks first described as the error tolerance of networks (65). If we remove the nodes from a network in a targeted manner, the spreading on the network could be quickly slowed down or

332 stopped. As it was demonstrated, the rapid spread of diseases is caused by the fact that there is a large  
 333 variance in the degrees of the nodes in these networks ( $\langle k^2 \rangle \gg \langle k \rangle$ ), and this comes from the  
 334 presence of hubs. If we want to decrease the variance (thus increasing  $\lambda_c$ ), we have to block hubs  
 335 from interacting.

### 336 *Selective sampling*

337 If we don't know the exact mapping of the contact network, we could reach for the 'friendship  
 338 paradox' (66) and the immunization strategy based on it proposed by Cohen et al. (67). The  
 339 friendship paradox says that on average the neighbours of a node have higher degrees than the node  
 340 itself. The average degree of a node's neighbour doesn't equal to  $\langle k \rangle$ , but it is a different number,  
 341 depending largely also on  $\langle k^2 \rangle$  (25). The origin of this phenomenon is that it is more likely for a  
 342 random node to be connected to a hub than to a small degree node, because hubs have more  
 343 connections than other nodes. Thus, immunizing (or isolating) the contacts of randomly selected  
 344 individuals, we target the hubs without knowing exactly which individuals are the hubs.

### 345 *Targeted sampling*

346 If we knew the whole contact network, we could target the most prominent hubs. We don't know the  
 347 exact mapping of the Hungarian social network, but we can have the following assumptions:

- 348 - The network is scale-free;
- 349 - where the probability  $p_k$  that a node has exactly  $k$  links is:  $p_k = \frac{k^{-\gamma}}{\xi(\gamma)}$ , where  $\gamma$  is the degree  
 350 exponent and  $\xi(\gamma)$  is the Riemann-zeta function (using discrete formalism (25));
- 351 - and  $2 < \gamma < 3$ , as in most of real-life networks.

352 With targeted sampling we try to remove all nodes whose degree is larger than  $k_t$ . From an  
 353 epidemiological viewpoint this is the same as removing the high degree nodes from the network with  
 354 their links as well. With this intervention, the network will change, and  $\lambda_c$  will increase (25):

$$355 \quad \lambda'_c = \left[ \frac{\gamma-2}{3-\gamma} k_t^{3-\gamma} k_{min}^{\gamma-2} - \frac{\gamma-2}{3-\gamma} k_t^{5-2\gamma} k_{min}^{2\gamma-4} + k_t^{2-\gamma} k_{min}^{\gamma-2} - 1 \right]^{-1} \quad (6)$$

356 Depending on the degree exponent, and setting  $k_{min}$  to 1, we could obtain target degrees ( $k_t$ ) with the  
 357 new epidemic thresholds ( $\lambda'_c$ ).

358

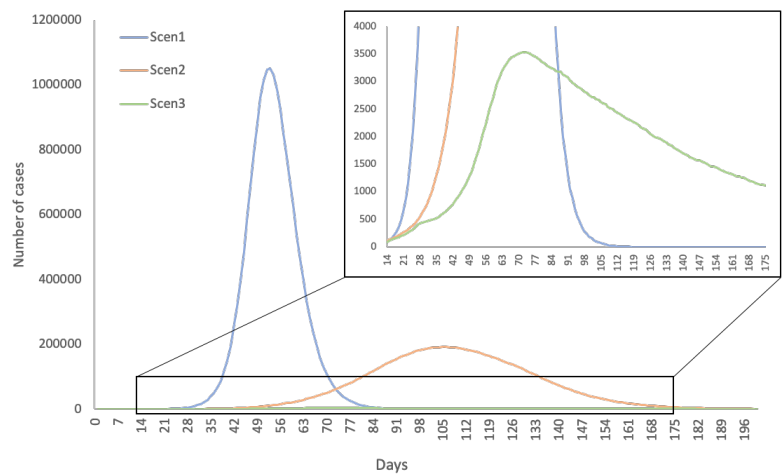
## 359 **Results**

### 360 **Results of epidemiological modelling**

361 Different scenarios were run in the publicly available version of GLEAMviz software with the  
 362 settings described in 'Methods' section. As the software only provides the number and cumulative  
 363 number of new transitions of individuals per 1000 people regarding one compartment to another in a  
 364 daily breakdown, an algorithm was developed in KNIME software (63) in order to automatically  
 365 convert the GLEAMviz outputs into actual daily case numbers of different compartments.

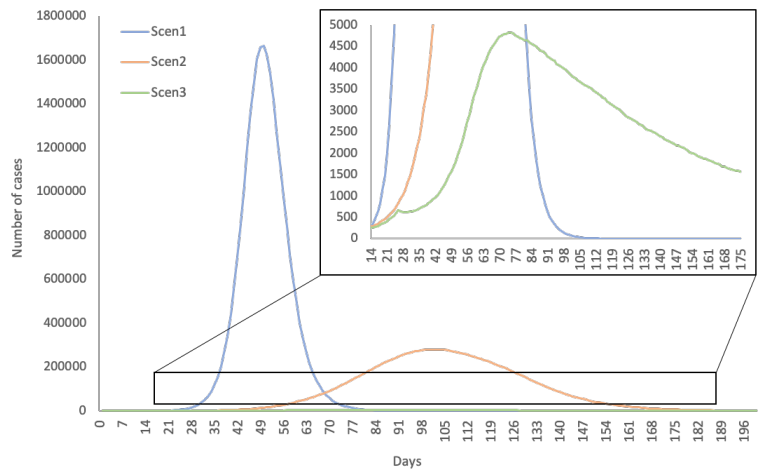
Figures 2 and 3 show the comparison of distribution of Infected and Exposed (latent) individuals in different scenarios.

Figure 2



Distribution of Infected individuals in *Scenarios 1 to 3*

Figure 3



Distribution of Exposed (latent) individuals in *Scenarios 1 to 3*.

The proportion of maximally affected latent and infected people (daily and overall) can be seen in Table 5. According to the modelling, about 1,000,000; 190,000 and 3,500 people will be infected on the day, when the epidemic reaches its peak in *Scenarios 1, 2 and 3*, respectively. Overall, about 5,400,000; 3,300,000 and 110,000 people will get through the infection with moderate or serious symptoms in *Scenarios 1, 2 and 3* and respectively. Note that in case of Scenario 3, the maximum number was not reached till the end of the simulation (365 days, which was the limitation of the software).

Table 5. Proportion of maximum number of daily and cumulated cases of infected and latent people in Hungary.

		Proportion in the population <sup>1</sup> (median with LCL <sup>2</sup> and UCL <sup>3</sup> ) (%)		No. of days <sup>4</sup>
<b>Scenario 1</b>	Maximum of daily cases	Infected	11.42 (7.99-12.62)	52
		Latent	18.07 (12.51-20.29)	49
	Maximum of cumulated cases	Infected	58.69 (58.65-58.72)	118
		Latent	93.89 (93.85-93.91)	122
<b>Scenario 2</b>	Maximum of daily cases	Infected	2.08 (1.76-2.38)	105
		Latent	3.05 (2.57-3.05)	101
	Maximum of cumulated cases	Infected	35.89 (35.82-35.94)	268
		Latent	57.36 (57.26-57.42)	279
<b>Scenario 3</b>	Maximum of daily cases	Infected	0.04 (0.04-0.04)	72
		Latent	0.05 (0.05-0.06)	74
	Maximum of cumulated cases	Infected	1.22 (1.12-1.31)	365*
		Latent	1.85 (1.69-2.00)	365*

as 9,213,366 people

<sup>2</sup>: Lower confidence limit originating from the 20 different simulations

<sup>3</sup>: Upper confidence limit originating from the 20 different simulations

<sup>4</sup>: Regarding median value

\*: Maximum number was not reached till the end of the simulation (365 days, which was the limitation of the software)

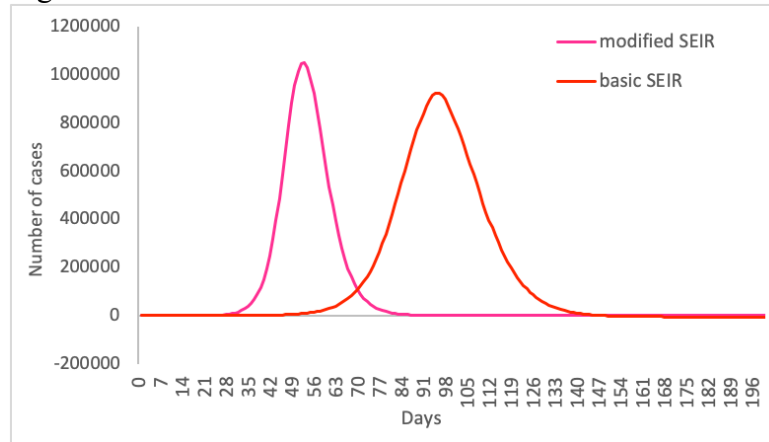
Regarding exposed (latent) people, who will only have mild symptoms or no symptoms at all (according to our assumption), on the day of the peak of the epidemic, about 1,700,000; 280,000 and 4,800 people will be affected in *Scenarios 1, 2 and 3*, respectively. Overall, about 8,700,000; 5,300,000 and 170,000 people will get through the infection with mild symptoms or as asymptomatic cases in *Scenarios 1, 2 and 3*, respectively. The same limitation in case of Scenario 3 applies here as well regarding the maximum number of latent people.

Note that the modelling is a robust estimate for actual case numbers, therefore only approximate values are indicated.

### Comparison of modified SEIR model with traditional SEIR model

Basic SEIR model results in somewhat lower number of daily infections, daily latent cases, and cumulative latent cases (1.38%, 3.07%, and 1.74%, respectively) but overall, the cumulative number of infectious individuals are 33.47% higher compared to the modified SEIR model (Table 6). It can be seen that the peak of the curve is shifted in the basic SEIR model (from about 50 days after the start date of the simulation to the ~90<sup>th</sup> day) (Fig. 4.).

Figure 4



Comparison of the distribution of Infected individuals in case of modified SEIR model and basic SEIR model in case of *Scenario 1*

Table 6. Proportion of maximum number of daily and cumulated cases of infected and latent people in modified SEIR model compared with basic SEIR model Settings of Scenario 1 was applied.

		Modified SEIR model		Basic SEIR model	
		Proportion in the population <sup>1</sup> (median with LCL <sup>2</sup> and UCL <sup>3</sup> ) (%)	No. of days <sup>4</sup>	Proportion in the population <sup>1</sup> (median with LCL <sup>2</sup> and UCL <sup>3</sup> ) (%)	No. of days <sup>4</sup>
Maximum no. of daily cases	Infected	11.42 (7.99-12.62)	52	10.04 (8.01-10.89)	95
	Latent	18.07 (12.51-20.29)	49	15.00 (11.61-16.68)	91
Maximum no. of cumulated cases	Infected	58.69 (58.65-58.72)	118	92.16 (92.10-92.22)	214
	Latent	93.89 (93.85-93.91)	122	92.15 (92.10-92.20)	211

<sup>1</sup>: Population of Hungary registered in GLEAMviz was 9,213,366 people

<sup>2</sup>: Lower confidence limit originating from the 20 different simulations

<sup>3</sup>: Upper confidence limit originating from the 20 different simulations

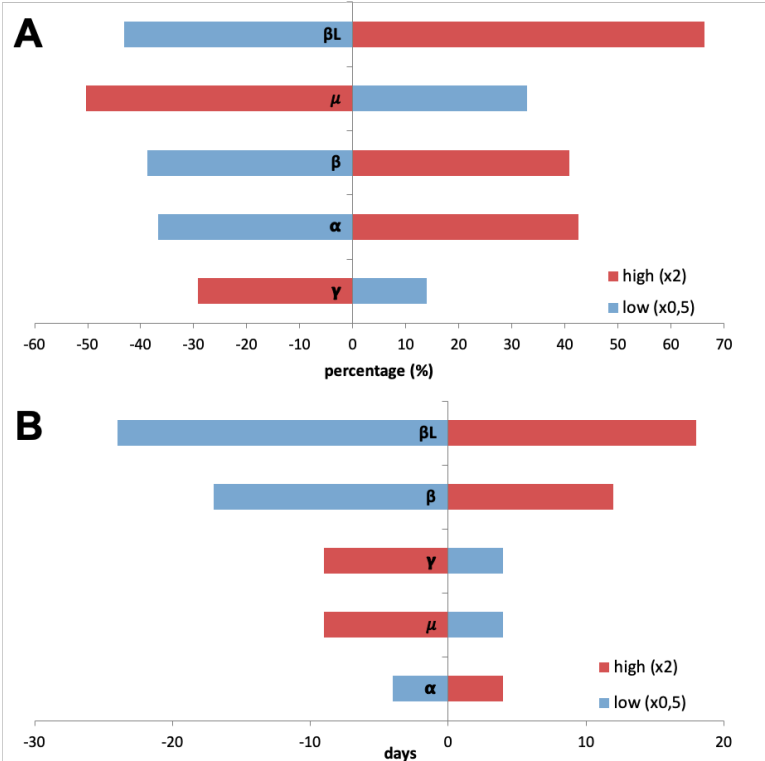
<sup>4</sup>: Regarding median value

## Sensitivity analysis of modified SEIR model

Most pronounced changes in both chosen endpoints can be seen in case of  $\beta_L$ , increasing its value by 2 times resulted in a ~66% increase in the number of maximum daily infections (Fig. 5A), and decreasing its value to the half of the original ended up in a 24 days sooner peak in the curve of the number of daily infections (Fig. 5B). However, other the importance of parameters such as  $\mu$  and  $\beta$  are also indicated by the tornado-plot.

424

Figure 5



Results of sensitivity analysis of the modified SEIR model: changes in daily maximum value of individuals in the infected compartment (A) and changes in the number of the days related to the former endpoint (B)

425

426

427

428

429

430 **Results of network analysis**

431 To address the problem caused by the inability of conventional compartment models to capture the  
432 non-homogenous nature of the population, network-based analyses were also performed, which  
433 yielded the following results.

434 Based on the Copenhagen Networks Study (60) data, we found average degree  $\langle k \rangle = 46$ , the second  
435 moment of the degree  $\langle k^2 \rangle = 2847$  and based on Equation (4) the epidemic threshold  $\lambda_c = 0.016$ . Basic  
436 parameters of modified SEIR model (*Scenario 1*) was set to be in line with the average  $R_0$  value of  
437 3.1 of Read et al. (32) and Tian et al. (33). Using Equation (3), the spreading rate of the virus was  
438  $\lambda = 0.067$ , which means that for stopping the epidemic, we need to change the network in such a way  
439 that  $\lambda_c$  will be increased above this value.

440 *Random sampling*

441 In case of random sampling, testing (and consequent removing of SARS-CoV-2 positive people from  
442 the contact network), based on equation (5) we have found the critical immunization to be  $g_c = 0.761$ .  
443 This means that 76.1% of the population shall be removed from the network. This implies very strict  
444 sampling and quarantine measures with testing a very large proportion of the population.

445 *Selective sampling*



446 Using the ‘friendship paradox’, the procedure proposed by Cohen et al. (67), consists of three steps:

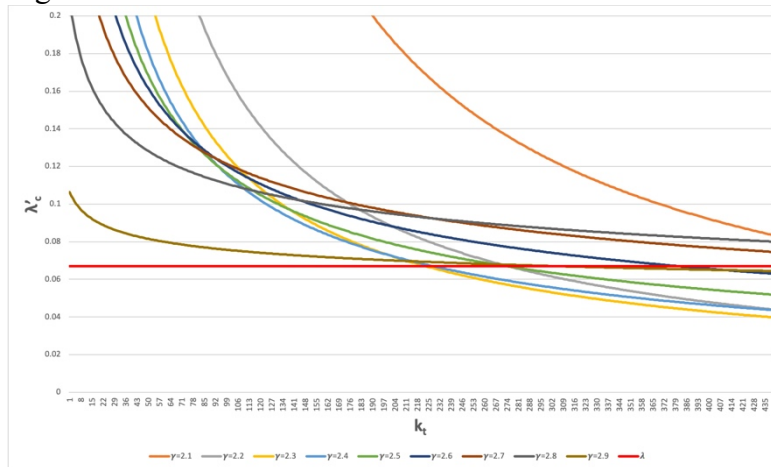
- 447 1. Choosing randomly a fraction of nodes, this is layer 0.
- 448 2. Selecting randomly a link for each node in layer 0. The nodes to which these links connect will
- 449 form layer 1.
- 450 3. Immunizing (in our case sampling and testing) the layer 1 individuals.

451 This sampling strategy doesn’t require information on the structure of the network. According to  
 452 Cohen et al. (67),  $g_c$  is systematically under 0.3. It means that by selecting and removing a randomly  
 453 chosen neighbour of 30% of the population, the spreading of the disease could be stopped. With  
 454 selecting contacts referred simultaneously by more people, this strategy could be even enhanced.

### 455 *Targeted sampling*

456 With targeted sampling we try to remove all nodes whose degree is larger than  $k_t$ . Based on equation  
 457 (6), we could obtain target degrees ( $k_t$ ) with the new epidemic thresholds ( $\lambda'_c$ ) which are presented on  
 458 Figure 6. The figure shows target degrees  $k_t$  in the range of 234 (for  $\gamma=2.3$ ) to  $>1000$  (for  $\gamma=2.8$ ),  
 459 meaning that if we could sample (and then contain all positive cases) the super-spreaders with contact  
 460 number above 234, the epidemic threshold would be high enough to stop the disease.

461 **Figure 6**



462 Epidemic thresholds ( $\lambda'_c$ ) of different degree exponents ( $\gamma$ ) and target  
 463 degrees ( $k_t$ ) calculated to increase the epidemic threshold above the  
 464 spreading rate of COVID-19 with targeted sampling. The spreading rate  
 465 ( $\lambda$ ) of the virus is set to 0.067 (red line).  
 466

467 How does it translate to the Hungarian population? Idealizing a scale-free network, the number of  
 468 people with contacts  $k \geq k_t$  can be calculated with (25):

$$469 \quad N_{k \geq k_t} = N \sum_{k=k_t}^{\infty} \frac{k^{-\gamma}}{\xi(\gamma)} \quad (8)$$

470 Setting  $\gamma=2.3$  and  $k_t=234$ , this is in the magnitude of 0.04% of the population only.

471

## 472 **Discussion**

473

## 474 Potentials and limitations of the modelling

475 Scenarios have been designed to simulate the most likely spread of COVID-19 in Hungary with no  
476 interventions (*Scenario 1*) and the effect of actually applied interventions (*Scenarios 2 and 3*) in  
477 order to gain information on the effect of intervention measures on the disease spreading. According  
478 to the results, the applied interventions (social distancing and hygienic measures) have a great impact  
479 on the disease spreading and are effective in controlling the COVID-19 epidemic (*Scenario 3*).

480 The main advantage of epidemiological modelling with GLEAMviz software is that besides the  
481 characteristic parameters of the infectious disease, other essential factors are taken into account when  
482 simulating the disease spreading, namely population density and mobility of the population. The  
483 irregular network structure, that affects the local spread of infectious disease between neighbouring  
484 subpopulations is captured in GLEAMviz datasets, so as the difference between high traffic and low  
485 traffic airports that has a significant impact of disease spreading around the globe.

486 Simulations are evaluated for the Hungarian region, but with GLEAMviz, it is possible to set the  
487 initial number of infected individuals in different cities on the day when the simulation starts, thereby  
488 the impact of global presence of infected people is also taken into account. Note that registered  
489 number of infected people in different countries/cities carries bias as the protocol for registering  
490 COVID-19 positive cases and number of tests performed differ greatly from country to country.  
491 Nonetheless, these data and this option provide additional adjustable settings that contributes to more  
492 realistic simulations.

## 493 Evaluation of modified SEIR model – sensitivity analysis

494 All modelling has their limitations, and this applies particularly to modelling of emerging diseases  
495 such as COVID-19. As limited data are available regarding SARS-CoV-2 and the spread of COVID-  
496 19, parameters of the compartment model can only be estimated. Our modified SEIR model has been  
497 made by using available data from scientific literature regarding the compartment model parameters  
498 and its novelty is that the route of infection transmission from the Exposed compartment (latent  
499 individuals) is built in. Compared to the traditionally applied SEIR model, in which latent individuals  
500 cannot transmit the infection to susceptible people, it results in an earlier and higher peak in the  
501 epidemic curve of infected individuals, which means a faster epidemic course with more infected  
502 people in shorter period of time, that poses greater burden to the healthcare system. However, total  
503 number of infections are lower altogether in the modified model compared to the basic SEIR model.  
504 According to this result, the experienced characteristics of COVID-19 epidemics, namely the so-  
505 called ‘exponential growth’ of the disease spread can be explained by the disease transmission of  
506 latent people in case of SARS-CoV-2. Sensitivity analysis of the modified SEIR model also reveals  
507 the importance of the disease transmission by latent individuals. According to the results, disease  
508 transmission related to latent individuals has the greatest impact on the results of the simulation  
509 regarding the number of maximum daily infections and the time of the peak of the epidemic.

## 510 Evaluation of network analysis results

511 When taking into account the social contact network topology during intervention planning, we have  
512 to be aware of the specific challenges and also opportunities these network characteristics pose. Most  
513 of the counterintuitive network phenomena are caused by the presence of hubs, i.e. nodes with large  
514 amount of contacts, which could also be identified as super-spreaders. One of the results is that the  
515 diseases spread much faster on real networks than conventional compartment models would predict.  
516 This also means that the  $R_0$  identified as a benchmark value might be wrong: even if  $R_0 < 1$ , there

517 might be still nodes in the network whose degree is higher than the average degree, maintaining and  
518 spreading the disease.

519 The usual intervention strategies mentioned in this paper are still useful and effective, but they don't  
520 target the super-spreader hubs. When planning sampling strategies, *random sampling* would imply  
521 very strict sampling and quarantine measures with testing a very large proportion of the population  
522 (>75%). When the 'friendship paradox' (i.e. on average the neighbours of a node have higher degree  
523 than the node itself) would be used for planning *selective sampling*, a significantly lower number of  
524 samples (~30%) would suffice. And if we could find the super-spreader hubs in a network during  
525 *targeted sampling*, <1% of the population would be enough to be sampled, tested and isolated.

526 Of course, natural contact networks are not ideal scale-free networks, and we don't know the exact  
527 super-spreaders either. Nevertheless, according to the recent analysis of the Hungarian Centre for  
528 Economic and Regional Studies Institute of Economics on occupations affected the most by the  
529 COVID-19 outbreak (69) 18% of the people are working in these occupational areas. These include  
530 healthcare and social workers, retail and restaurant workers, drivers, cleaning staff, pharmacists,  
531 veterinarians, public transport workers, postmen and waste removal staff. If the targeted sampling  
532 strategy would aim for these occupations, with strict quarantine measures of the positive cases, the  
533 spreading of the virus could be significantly slowed down.

## 534 **Conclusion**

### 535 **Comparison with real COVID-19 epidemiological situation in Hungary**

536 The first wave of the disease spreading, according to the reported COVID-19 cases in Hungary,  
537 SARS-CoV-2 have not caused a great epidemic in Hungary Multiple reasons can explain this, some  
538 of them are listed hereunder.

- 539 • By the time the epidemic reached Hungary, there were several frightening scenarios (massive  
540 amount of infections and deaths caused by COVID-19 in China, Italy etc.) that warned the  
541 public and raised the awareness for caution about COVID-19 and discipline regarding social  
542 distancing and hygiene. People have started to draw each other's attention through social  
543 media and encouraged staying at home, therefore social distancing have started even earlier  
544 and have been applied stricter than the actual measurements of the Hungarian government  
545 required.
- 546 • Because of conscious social distancing, super-spreading events have been prevented in the  
547 very early phase of the epidemic, which has a great impact on the fate of later number of  
548 infections (59).
- 549 • Many studies investigate the association of Bacillus Calmette-Guérin (BCG) vaccination with  
550 reduced morbidity and mortality of COVID-19 (70,71). In Hungary, BCG vaccination is  
551 compulsory since 1954, therefore BCG vaccination coverage is very high. This can also  
552 contribute to the low number of COVID-19 infections in Hungary.

553 Our modelling results show a good correlation with the results of the Hungarian CoronaVirus  
554 disease-19 Epidemiological Research(72). H-UNCOVER was a large-scale, cross-sectional,  
555 representative population screening of Hungarian male or female patients aged 14 and over who live  
556 in private households, aiming for sampling and investigating the rate of the infected patients,  
557 asymptomatic carrier and healed patients (48). According of the extrapolation of the results of 10,575

558 patients sampled between 1-16 May 2020, there were 2,421 active cases in Hungary and 56,439  
559 people were asymptomatic carriers and healed patients.

560 According to the results of our modelling in *Scenario 3*, there were 3,527 active infected cases on day  
561 70 (12<sup>th</sup> May) and 38,692 cumulative recovered people by day 70 and 4,756 active latent cases on  
562 day 70, adding up to 43,448 asymptomatic carriers and healed patients.

563

#### 564 **Proposal for disease control with agile, risk-based testing**

565 Our study proposes a long-term feasible risk-based approach for testing SARS-CoV-2 infections, that  
566 could gradually replace isolation interventions by the early detection of positive cases between the  
567 so-called 'super-spreaders', thereby preventing mass infections and breaking infection chains with  
568 removing the seed of the infection in a timely manner. In cases when number of positive cases tend  
569 to increase nonetheless of the quarantine of affected people, social isolation measures can be re-  
570 initiated in a timely manner and epidemic crisis can thereby be prevented.

571 With the help of network analysis, people can be grouped into risk categories regarding SARS-CoV-  
572 2 transmission. In this case, the key parameter for establishing risk categories is the number of  
573 physical interactions between people. A continuous testing is suggested but with the allocation of  
574 resources (test kits, testing personnel, financial resources) to the high-risk groups. People could be  
575 categorized by risk scores of physical interactions based on their occupation. Occupations like  
576 healthcare and social workers, retail and restaurant workers, drivers, cleaning staff, pharmacists,  
577 veterinarians, public transport workers, postmen and waste removal staff would fall into this high-  
578 risk group. These people must be tested much more often as they play key role in SARS-CoV-2  
579 transmission. From this group, healthcare workers could be identified as key actors from network  
580 perspective, implying even stricter sampling and testing regime for them. When identified positive  
581 cases of super-spreaders would be isolated, this would have a large effect on the contact network  
582 itself, cutting off all the links of the large hubs, thus slowing down the spreading considerably.

583 Our approach is generally applicable for the prevention and early detection of epidemics caused by  
584 other microorganisms as well, thereby protecting human health and preventing economic crises  
585 caused by emerging and re-emerging diseases.

#### 586 **Proposal for data collection and data sharing**

587 Our study also points to the well-known fact that models are only as good as their input data. When  
588 modelling and planning intervention strategies, fit-for-purpose and timely data are essential. Using  
589 specific population like college student data can't be used for precise modelling of the spreading of  
590 diseases in other societal groups. Unfortunately, there is a lack of social contact data with sufficient  
591 granularity, and advances on network science couldn't be fully exploited in real-life situations. It is  
592 not to say that collecting and sharing contact network data for public health purposes would  
593 overwrite data protection and privacy aspects, but as Oliver et al. (73) pointed out, there are available  
594 data sources like mobile phone data, which could be extremely useful for such purposes. These  
595 datasets, if would be made available in a careful and transparent manner and taking into account data  
596 protections issues, could also be used for other important public health domains, like foodborne  
597 disease outbreak investigation.

598 In our paper we had two important objectives regarding network analysis approach to  
599 epidemiological modelling:

- 600 - Showing the profound implications of network theory for epidemiological modelling and risk  
601 management, since the network epidemiological approach is not widely known in the public  
602 health community. Most of the analyses and also intervention strategies don't take into  
603 account the inhomogeneity of the connections nor the network-based background of the  
604 spreading of the virus. Even when there is a general knowledge on the role of super-spreaders,  
605 the quantification of this role is not well known.
- 606 - Network analysis (but also all computational science methods) need large amount of good  
607 quality data and the spread of these methods could be supported by easy-to-use tools. We  
608 wanted to raise awareness also on this issue.

609 These two objectives are in close connection, since the lack of fit-for-purpose data and access to  
610 computational methods prevent the public health community from applying network-based approach  
611 in the decision-making process. However, the public health community should work towards solving  
612 data and tool related issues, for example with using proxy data in a short term (e.g. mobile phone  
613 data, tracing applications, etc.) or with planned exercises on network data collection in the long run.

614

## 615 **Declaration**

616 Ethics approval and consent to participate  
617 Not applicable.

618  
619 Consent for publication  
620 The authors consent for publication.

621  
622 Availability of data and materials  
623 All the analysed and generated data during this study are included and referred in this published  
624 article. The KNIME workflow is available at [https://univet.hu/en/research/dfi/publications/scientific-](https://univet.hu/en/research/dfi/publications/scientific-publications/covid-19/)  
625 [publications/covid-19/](https://univet.hu/en/research/dfi/publications/scientific-publications/covid-19/).

626  
627 Competing interests  
628 The authors declare no competing interests.

629  
630 Funding  
631 Not applicable.

632  
633 Author Contributions  
634 ZSF prepared the modelling and wrote the main body of the text; ÁJ created the concept of the  
635 network study and prepared the related research; TE and ZSF prepared the tables; SZCS prepared the  
636 figures; MS, EO, SZCS, TE and ZSF did the literature research; MS reviewed the first draft of the  
637 manuscript. TE prepared the sensitivity analysis. All authors contributed to the creation of the  
638 epidemiological compartment model in the study and the concept of the research. All authors  
639 contributed to manuscript revision, read and approved the version to be submitted

640

641 Acknowledgement  
642 Not applicable.

643 **References**

- 644 1. Zhou P, Yang X-L, Wang X-G, Hu B, Z. hang L, Zhang W, et al. A pneumonia outbreak  
645 associated with a new coronavirus of probable bat origin. *Nature*. 2020 Mar 12;579(7798):270–3.
- 646 2. Zheng J. SARS-CoV-2: an Emerging Coronavirus that Causes a Global Threat. *Int J Biol Sci*.  
647 2020;16(10):1678–85.
- 648 3. Coronaviridae Study Group of the International Committee on Taxonomy of Viruses. The species  
649 Severe acute respiratory syndrome-related coronavirus: classifying 2019-nCoV and naming it  
650 SARS-CoV-2. *Nat Microbiol*. 2020 Apr;5(4):536–44.
- 651 4. WHO. Naming the coronavirus disease (COVID-19) and the virus that causes it [Internet]. 2020.  
652 Available from: [https://www.who.int/emergencies/diseases/novel-coronavirus-2019/technical-](https://www.who.int/emergencies/diseases/novel-coronavirus-2019/technical-guidance/naming-the-coronavirus-disease-(covid-2019)-and-the-virus-that-causes-it)  
653 [guidance/naming-the-coronavirus-disease-\(covid-2019\)-and-the-virus-that-causes-it](https://www.who.int/emergencies/diseases/novel-coronavirus-2019/technical-guidance/naming-the-coronavirus-disease-(covid-2019)-and-the-virus-that-causes-it)
- 654 5. Singhal T. A Review of Coronavirus Disease-2019 (COVID-19). *Indian J Pediatr*. 2020  
655 Apr;87(4):281–6.
- 656 6. Cascella M, Rajnik M, Cuomo A, Dulebohn SC, Di Napoli R. Features, Evaluation, and  
657 Treatment of Coronavirus. In: *StatPearls* [Internet]. Treasure Island (FL): StatPearls Publishing;  
658 2020 [cited 2020 Nov 25]. Available from: <http://www.ncbi.nlm.nih.gov/books/NBK554776/>
- 659 7. van Doremalen N, Bushmaker T, Morris DH, Holbrook MG, Gamble A, Williamson BN, et al.  
660 Aerosol and surface stability of HCoV-19 (SARS-CoV-2) compared to SARS-CoV-1 [Internet].  
661 *Infectious Diseases (except HIV/AIDS)*; 2020 Mar [cited 2020 Nov 25]. Available from:  
662 <http://medrxiv.org/lookup/doi/10.1101/2020.03.09.20033217>
- 663 8. Cai J, Sun W, Huang J, Gamber M, Wu J, He G. Indirect Virus Transmission in Cluster of  
664 COVID-19 Cases, Wenzhou, China, 2020. *Emerg Infect Dis*. 2020 Jun;26(6):1343–5.
- 665 9. Jia J, Ding J, Liu S, Liao G, Li J, Duan B, et al. Modeling the Control of COVID-19: Impact of  
666 Policy Interventions and Meteorological Factors. *arXiv:200302985 [math, q-bio]* [Internet]. 2020  
667 Mar 5 [cited 2020 Nov 25]; Available from: <http://arxiv.org/abs/2003.02985>
- 668 10. Koo JR, Cook AR, Park M, Sun Y, Sun H, Lim JT, et al. Interventions to mitigate early spread of  
669 SARS-CoV-2 in Singapore: a modelling study. *The Lancet Infectious Diseases*. 2020  
670 Jun;20(6):678–88.
- 671 11. Peng L, Yang W, Zhang D, Zhuge C, Hong L. Epidemic analysis of COVID-19 in China by  
672 dynamical modeling [Internet]. *Epidemiology*; 2020 Feb [cited 2020 Nov 25]. Available from:  
673 <http://medrxiv.org/lookup/doi/10.1101/2020.02.16.20023465>
- 674 12. Shen M, Peng Z, Xiao Y, Zhang L. Modeling the Epidemic Trend of the 2019 Novel Coronavirus  
675 Outbreak in China. *The Innovation*. 2020 Nov;1(3):100048.

13. Li D, Liu Z, Liu Q, Gao Z, Zhu J, Yang J, et al. Estimating the Efficacy of Quarantine and Traffic Blockage for the Epidemic Caused by 2019-nCoV (COVID-19):A Simulation Analysis [Internet]. *Epidemiology*; 2020 Feb [cited 2020 Nov 25]. Available from: <http://medrxiv.org/lookup/doi/10.1101/2020.02.14.20022913>
14. Peak CM, Kahn R, Grad YH, Childs LM, Li R, Lipsitch M, et al. Modeling the Comparative Impact of Individual Quarantine vs. Active Monitoring of Contacts for the Mitigation of COVID-19 [Internet]. *Infectious Diseases (except HIV/AIDS)*; 2020 Mar [cited 2020 Nov 25]. Available from: <http://medrxiv.org/lookup/doi/10.1101/2020.03.05.20031088>
15. Ferguson N, Laydon D, Nedjati Gilani G, Imai N, Ainslie K, Baguelin M, et al. Report 9: Impact of non-pharmaceutical interventions (NPIs) to reduce COVID19 mortality and healthcare demand [Internet]. Imperial College London; 2020 Mar [cited 2020 Nov 25]. Available from: <http://spiral.imperial.ac.uk/handle/10044/1/77482>
16. Tang Z, Li X, Li H. Prediction of New Coronavirus Infection Based on a Modified SEIR Model. *medRxiv* [Internet]. 2020 Mar 6; Available from: <https://www.medrxiv.org/content/10.1101/2020.03.03.20030858v1>
17. Flaxman S, Mishra S, Gandy A, Unwin H, Coupland H, Mellan T, et al. Report 13: Estimating the number of infections and the impact of non-pharmaceutical interventions on COVID-19 in 11 European countries [Internet]. Imperial College London; 2020 Mar [cited 2020 Nov 25]. Available from: <http://spiral.imperial.ac.uk/handle/10044/1/77731>
18. Wu JT, Leung K, Leung GM. Nowcasting and forecasting the potential domestic and international spread of the 2019-nCoV outbreak originating in Wuhan, China: a modelling study. *Lancet*. 2020 Jan 31;395:689–97.
19. Li R, Pei S, Chen B, Song Y, Zhang T, Yang W, et al. Substantial undocumented infection facilitates the rapid dissemination of novel coronavirus (SARS-CoV-2). *Science*. 2020 May 1;368(6490):489–93.
20. Mizumoto K, Kagaya K, Zarebski A, Chowell G. Estimating the asymptomatic proportion of coronavirus disease 2019 (COVID-19) cases on board the Diamond Princess cruise ship, Yokohama, Japan, 2020. *Eurosurveillance* [Internet]. 2020 Mar 12 [cited 2020 Nov 25];25(10). Available from: <https://www.eurosurveillance.org/content/10.2807/1560-7917.ES.2020.25.10.2000180>
21. Nishiura H, Kobayashi T, Miyama T, Suzuki A, Jung S-M, Hayashi K, et al. Estimation of the asymptomatic ratio of novel coronavirus infections (COVID-19). *Int J Infect Dis*. 2020;94:154–5.
22. Du Z, Xu X, Wu Y, Wang L, Cowling BJ, Meyers LA. Serial Interval of COVID-19 among Publicly Reported Confirmed Cases. *Emerg Infect Dis*. 2020 Jun;26(6):1341–3.
23. Ganyani T, Kremer C, Chen D, Torneri A, Faes C, Wallinga J, et al. Estimating the generation interval for coronavirus disease (COVID-19) based on symptom onset data, March 2020. *Eurosurveillance* [Internet]. 2020 Apr 30 [cited 2020 Nov 25];25(17). Available from: <https://www.eurosurveillance.org/content/10.2807/1560-7917.ES.2020.25.17.2000257>

714 24. Chisholm RH, Campbell PT, Wu Y, Tong SYC, McVernon J, Geard N. Implications of  
715 asymptomatic carriers for infectious disease transmission and control. *R Soc open sci.* 2018  
716 Feb;5(2):172341.

717 25. Barabási A-L, Pósfai M. *Network science*. Cambridge, United Kingdom: Cambridge University  
718 Press; 2016. 456 p.

719 26. WHO. Statement on the first meeting of the International Health Regulations (2005) Emergency  
720 Committee regarding the outbreak of novel coronavirus (2019-nCoV) [Internet]. 2020. Available  
721 from: [https://www.who.int/news/item/23-01-2020-statement-on-the-meeting-of-the-international-](https://www.who.int/news/item/23-01-2020-statement-on-the-meeting-of-the-international-health-regulations-(2005)-emergency-committee-regarding-the-outbreak-of-novel-coronavirus-(2019-ncov))  
722 [health-regulations-\(2005\)-emergency-committee-regarding-the-outbreak-of-novel-coronavirus-](https://www.who.int/news/item/23-01-2020-statement-on-the-meeting-of-the-international-health-regulations-(2005)-emergency-committee-regarding-the-outbreak-of-novel-coronavirus-(2019-ncov))  
723 [health-regulations-\(2005\)-emergency-committee-regarding-the-outbreak-of-novel-coronavirus-](https://www.who.int/news/item/23-01-2020-statement-on-the-meeting-of-the-international-health-regulations-(2005)-emergency-committee-regarding-the-outbreak-of-novel-coronavirus-(2019-ncov))  
(2019-ncov)

724 27. Tang B, Wang X, Li Q, Bragazzi NL, Tang S, Xiao Y, et al. Estimation of the Transmission Risk  
725 of the 2019-nCoV and Its Implication for Public Health Interventions. *JCM.* 2020 Feb  
726 7;9(2):462.

727 28. Liu T, Hu J, Xiao J, He G, Kang M, Rong Z, et al. Time-varying transmission dynamics of Novel  
728 Coronavirus Pneumonia in China [Internet]. *Systems Biology*; 2020 Jan [cited 2020 Nov 25].  
729 Available from: <http://biorxiv.org/lookup/doi/10.1101/2020.01.25.919787>

730 29. Li Q, Guan X, Wu P, Wang X, Zhou L, Tong Y, et al. Early Transmission Dynamics in Wuhan,  
731 China, of Novel Coronavirus–Infected Pneumonia. *N Engl J Med.* 2020 Mar 26;382(13):1199–  
732 207.

733 30. Linton NM, Kobayashi T, Yang Y, Hayashi K, Akhmetzhanov AR, Jung S-M, et al. Incubation  
734 Period and Other Epidemiological Characteristics of 2019 Novel Coronavirus Infections with  
735 Right Truncation: A Statistical Analysis of Publicly Available Case Data. *J Clin Med.* 2020 Feb  
736 17;9(2).

737 31. Lauer SA, Grantz KH, Bi Q, Jones FK, Zheng Q, Meredith HR, et al. The Incubation Period of  
738 Coronavirus Disease 2019 (COVID-19) From Publicly Reported Confirmed Cases: Estimation  
739 and Application. *Annals of Internal Medicine.* 2020 May 5;172(9):577–82.

740 32. Read JM, Bridgen JRE, Cummings DAT, Ho A, Jewell CP. Novel coronavirus 2019-nCoV: early  
741 estimation of epidemiological parameters and epidemic predictions [Internet]. *Infectious*  
742 *Diseases (except HIV/AIDS)*; 2020 Jan [cited 2020 Nov 25]. Available from:  
743 <http://medrxiv.org/lookup/doi/10.1101/2020.01.23.20018549>

744 33. Tian H, Liu Y, Li Y, Wu C-H, Chen B, Kraemer MUG, et al. An investigation of transmission  
745 control measures during the first 50 days of the COVID-19 epidemic in China. *Science.* 2020  
746 May 8;368(6491):638–42.

747 34. Patrozou E, Mermel LA. Does Influenza Transmission Occur from Asymptomatic Infection or  
748 Prior to Symptom Onset? *Public Health Rep.* 2009 Mar;124(2):193–6.

749 35. Longini IM. Containing Pandemic Influenza with Antiviral Agents. *American Journal of*  
750 *Epidemiology.* 2004 Apr 1;159(7):623–33.

751 36. GLEAMviz [Internet]. Available from: <http://www.gleamviz.org>



37. Broeck WV den, Gioannini C, Gonçalves B, Quaggitto M, Colizza V, Vespignani A. The GLEaMviz computational tool, a publicly available software to explore realistic epidemic spreading scenarios at the global scale. *BMC Infect Dis.* 2011 Dec;11(1):37.
38. Balcan D, Hu H, Goncalves B, Bajardi P, Poletto C, Ramasco JJ, et al. Seasonal transmission potential and activity peaks of the new influenza A(H1N1): a Monte Carlo likelihood analysis based on human mobility. *BMC Med.* 2009 Dec;7(1):45.
39. Balcan D, Gonçalves B, Hu H, Ramasco JJ, Colizza V, Vespignani A. Modeling the spatial spread of infectious diseases: The GLObal Epidemic and Mobility computational model. *Journal of Computational Science.* 2010 Aug;1(3):132–45.
40. Balcan D, Colizza V, Goncalves B, Hu H, Ramasco JJ, Vespignani A. Multiscale mobility networks and the spatial spreading of infectious diseases. *Proceedings of the National Academy of Sciences.* 2009 Dec 22;106(51):21484–9.
41. Simini F, González MC, Maritan A, Barabási A-L. A universal model for mobility and migration patterns. *Nature.* 2012 Apr;484(7392):96–100.
42. Google. Community Mobility Reports [Internet]. Google; 2020. Available from: <https://www.google.com/covid19/mobility/>
43. Waze. Waze Stats: Active Wazers in HU Budapest. [Internet]. Available from: <http://wazestats.com/active.php?city=7>
44. COVID-19 pandemic in Hungary [Internet]. Available from: [koronavirus.gov.hu](http://koronavirus.gov.hu)
45. OAG. Coronavirus airline schedules data. [Internet]. Official Aviation Guide; 2020. Available from: <https://www.oag.com/coronavirus-airline-schedules-data>
46. Ren Y, Ercsey-Ravasz M, Wang P, González MC, Toroczkai Z. Predicting commuter flows in spatial networks using a radiation model based on temporal ranges. *Nat Commun.* 2014 Dec;5(1):5347.
47. Monto AS, DeJonge PM, Callear AP, Bazzi LA, Capriola SB, Malosh RE, et al. Coronavirus Occurrence and Transmission Over 8 Years in the HIVE Cohort of Households in Michigan. *The Journal of Infectious Diseases.* 2020 Jun 16;222(1):9–16.
48. KSH. H-UNCOVER – Reprezentatív felmérés a koronavírus elleni küzdelemben – eredmények [Internet]. KSH; Available from: [http://www.ksh.hu/huncover\\_reprezentativ\\_felmeres\\_eredmenyek](http://www.ksh.hu/huncover_reprezentativ_felmeres_eredmenyek)
49. Official COVID19 Dashboard public information [Internet]. Federal Ministry Republic of Austria, Social Affairs, Health, Care and Consumer Protection; 2020. Available from: <https://info.gesundheitsministerium.at/?l=en>
50. COVID-19: epidemiological update of March 4, 2020. [Internet]. Public Health France; 2020 Mar. Available from: <https://www.santepubliquefrance.fr/dossiers/coronavirus-covid-19/coronavirus-chiffres-cles-et-evolution-de-la-covid-19-en-france-et-dans-le-monde#block-266156>

- 789 51. Coronavirus Disease 2019 (COVID-19) Daily Situation Report of the Robert Koch Institutue.  
790 [Internet]. Robert Koch Institutue; 2020 Mar. Available from:  
791 [https://www.rki.de/DE/Content/InfAZ/N/Neuartiges\\_Coronavirus/Situationsberichte/2020-03-](https://www.rki.de/DE/Content/InfAZ/N/Neuartiges_Coronavirus/Situationsberichte/2020-03-04-en.pdf?__blob=publicationFile)  
792 [04-en.pdf?\\_\\_blob=publicationFile](https://www.rki.de/DE/Content/InfAZ/N/Neuartiges_Coronavirus/Situationsberichte/2020-03-04-en.pdf?__blob=publicationFile)
- 793 52. Rosini. Cases tested people tested / tested cases [github] [Internet]. github; Available from:  
794 [https://github.com/pcm-dpc/COVID-19/blob/master/dati-regioni/dpc-covid19-ita-regioni-](https://github.com/pcm-dpc/COVID-19/blob/master/dati-regioni/dpc-covid19-ita-regioni-20200304.csv)  
795 [20200304.csv](https://github.com/pcm-dpc/COVID-19/blob/master/dati-regioni/dpc-covid19-ita-regioni-20200304.csv)
- 796 53. Report on confirmed COVID-19 cases in Spain. [Internet]. Carlos III. Health Institute; 2020 Mar.  
797 Available from: <https://cnecovid.isciii.es/covid19/#ccaa>
- 798 54. Iran COVID-19 death now 77 as emergency services chief infected. Channel New Asia  
799 [Internet]. 2020 Mar 4; Available from: [https://www.channelnewsasia.com/news/world/covid19-](https://www.channelnewsasia.com/news/world/covid19-coronavirus-death-toll-iran-77-mar-3-12496192)  
800 [coronavirus-death-toll-iran- 77-mar-3-12496192](https://www.channelnewsasia.com/news/world/covid19-coronavirus-death-toll-iran-77-mar-3-12496192)
- 801 55. Reustle S. Japan COVID-19 Coronavirus Tracker. [Internet]. Available from:  
802 <https://covid19japan.com>
- 803 56. MOH, Singapore. ONE MORE CASE DISCHARGED; TWO NEW CASES OF COVID-19  
804 INFECTION CONFIRMED [Internet]. Singapore: Ministry of Health; 2020 Mar. Available  
805 from: [https://www.moh.gov.sg/news-highlights/details/one-more-case-discharged-two-new-](https://www.moh.gov.sg/news-highlights/details/one-more-case-discharged-two-new-cases-of-covid-19-infection-confirmed)  
806 [cases-of-covid-19-infection-confirmed](https://www.moh.gov.sg/news-highlights/details/one-more-case-discharged-two-new-cases-of-covid-19-infection-confirmed)
- 807 57. No. of COVID-19 Cases in S. Korea Rises to 5,621 [Internet]. KBS World Radio; 2020 Mar.  
808 Available from: [http://world.kbs.co.kr/service/news\\_view.htm?lang=e&Seq\\_Code=151776](http://world.kbs.co.kr/service/news_view.htm?lang=e&Seq_Code=151776)
- 809 58. Pastor-Satorras R, Vespignani A. Epidemic Spreading in Scale-Free Networks. *Phys Rev Lett*.  
810 2001 Apr 2;86(14):3200–3.
- 811 59. Meyers LA, Pourbohloul B, Newman MEJ, Skowronski DM, Brunham RC. Network theory and  
812 SARS: predicting outbreak diversity. *Journal of Theoretical Biology*. 2005 Jan;232(1):71–81.
- 813 60. Sapiezynski P, Stopczynski A, Lassen DD, Lehmann S. Interaction data from the Copenhagen  
814 Networks Study. *Sci Data*. 2019 Dec;6(1):315.
- 815 61. WHO. Considerations for quarantine of contacts of COVID-19 cases [Internet]. 2020 Aug.  
816 Available from: [https://www.who.int/publications/i/item/considerations-for-quarantine-of-](https://www.who.int/publications/i/item/considerations-for-quarantine-of-individuals-in-the-context-of-containment-for-coronavirus-disease-(covid-19))  
817 [individuals-in-the-context-of-containment-for-coronavirus-disease-\(covid-19\)](https://www.who.int/publications/i/item/considerations-for-quarantine-of-individuals-in-the-context-of-containment-for-coronavirus-disease-(covid-19))
- 818 62. Stopczynski A, Pentland A ‘Sandy’, Lehmann S. How Physical Proximity Shapes Complex  
819 Social Networks. *Sci Rep*. 2018 Dec;8(1):17722.
- 820 63. Berthold MR, Cebon N, Dill F, Gabriel TR, Kötter T, Meinel T, et al. KNIME: The Konstanz  
821 Information Miner. In: Preisach C, Burkhardt H, Schmidt-Thieme L, Decker R, editors. *Data*  
822 *Analysis, Machine Learning and Applications*. Berlin, Heidelberg: Springer Berlin Heidelberg;  
823 2008. p. 319–26.
- 824 64. Csárdi G, Nepusz T. Igraph - The network analysis package [Internet]. 2006. Available from:  
825 <https://igraph.org>

- 826 65. Albert R, Jeong H, Barabási A-L. Error and attack tolerance of complex networks. *Nature*. 2000  
827 Jul 27;406(6794):378–82.
- 828 66. Feld SL. Why Your Friends Have More Friends Than You Do. *American Journal of Sociology*.  
829 1991 May;96(6):1464–77.
- 830 67. Cohen R, Havlin S, ben-Avraham D. Efficient Immunization Strategies for Computer Networks  
831 and Populations. *Phys Rev Lett*. 2003 Dec 9;91(24):247901.
- 832 68. Knime workflow [Internet]. Available from:  
833 <https://univet.hu/en/research/dfi/publications/scientific-publications/covid-19/>
- 834 69. Adamecz-Völgyi A, Szabó-Morvai Á. Kik dolgoznak a frontvonalban? [Internet]. MTA  
835 Közgazdaság- és Regionális Tudományi Kutatóközpontja; 2020 Apr. Available from:  
836 <https://www.mtakti.hu/koronavirus/kik-dolgoznak-a-frontvonalban/13090/>
- 837 70. Miller A, Reandelar MJ, Fasciglione K, Roumenova V, Li Y, Otazu GH. Correlation between  
838 universal BCG vaccination policy and reduced mortality for COVID-19. *medRxiv*. 2020 Sep 14;
- 839 71. Berg MK, Yu Q, Salvador CE, Melani I, Kitayama S. Mandated Bacillus Calmette-Guérin  
840 (BCG) vaccination predicts flattened curves for the spread of COVID-19 [Internet]. *Public and*  
841 *Global Health*; 2020 Apr [cited 2020 Nov 25]. Available from:  
842 <http://medrxiv.org/lookup/doi/10.1101/2020.04.05.20054163>
- 843 72. HUNgarian COronaVirus Disease-19 Epidemiological Research [Internet]. Semmelweis  
844 University Heart and Vascular Center; 2020 Jun. Available from:  
845 <https://clinicaltrials.gov/ct2/show/study/NCT04370067>
- 846 73. Oliver N, Lepri B, Sterly H, Lambiotte R, Deletaille S, De Nadai M, et al. Mobile phone data for  
847 informing public health actions across the COVID-19 pandemic life cycle. *Sci Adv*. 2020  
848 Jun;6(23):eabc0764.

849

## 1 Figure captions

Figure 1.

Structure of the modified SEIR model with compartment initials (Susceptible, Exposed (Latent), Infected, Recovered), transitions from one compartment to another (full line), parameters and routes of infection (dashed line). Susceptible individuals can get the infection either from individuals being in the Infected compartment with the rate of  $\beta$ , or from Exposed compartment (latent individuals) with the rate of  $\beta_L$ .

Figure 2.

Distribution of Infected individuals in *Scenarios 1* to *3*.

Figure 3.

Distribution of Exposed (latent) individuals in *Scenarios 1* to *3*.

Figure 4.

Comparison of the distribution of Infected individuals in case of modified SEIR model and basic SEIR model in case of *Scenario 1*.

Figure 5.

Results of sensitivity analysis of the modified SEIR model: changes in daily maximum value of individuals in the infected compartment (A) and changes in the number of the days related to the former endpoint (B)

Figure 6.

Epidemic thresholds ( $\lambda'_c$ ) of different degree exponents ( $\gamma$ ) and target degrees ( $k_t$ ) calculated to increase the epidemic threshold above the spreading rate of COVID-19 with targeted sampling. The spreading rate ( $\lambda$ ) of the virus is set to 0.067 (red line).